Incipient status of dyke intrusion in top crust – evidences from the Al-Ays 2009 earthquake swarm, Harrat Lunayyir, SW Saudi Arabia

Basab Mukhopadhyay , Saad Mogren , Manoj Mukhopadhyay & Sujit Dasgupta

Taylor & Francis
Taylor & Francis Group

Incipient status of dyke intrusion in top crust – evidences from the Al-Ays 2009 earthquake swarm, Harrat Lunayyir, SW Saudi Arabia

BASAB MUKHOPADHYAY*[†], SAAD MOGREN[‡],
MANOJ MUKHOPADHYAY[‡] and SUJIT DASGUPTA[§]

[†]Geological Survey of India, Central Headquarters, 27 J.L. Nehru Road, Kolkata 700016, India
[‡]Department of Geology & Geophysics, King Saud University, PO Box 2455, Riyadh 11451, Kingdom of Saudi Arabia
[§]Ex Geological Survey of India, Kolkata, India

The 2009 earthquake-swarm in the Al-Ays volcanic zone in Harrat-Lunayyir in NW Saudi-Arabia is unique because of its intense character and focal-depth distribution at two depth bands (5–10 and 15–20 km) in upper crust without volcanic eruption. We investigate an anatomy of the dyke-intrusion model that supports the mechanism for the swarm itself with seismotectonics, pore pressure diffusion process and inference model. Inferred dyke-intrusion initially started at depth had a five-day peak period (15–20 May 2009) since inception of event-recordings, following which the activity diminished. The process of pore pressure perturbation and resultant "r–t plot" with modelled diffusivity (D = 0.01) relates the diffusion of pore pressure to seismic sequence in a fractured poro-elastic fluid-saturated medium. The spatio-temporal b-values show high b-values (>1.3) along the zone of dyke intrusion (length 10 km and height 5 km) at $\sim$20km depth. The main-shock and other prominent earthquakes originated on a moderate b-value zone ($\sim$1.0). Temporal b-value analysis indicates an exceptionally low b-value ($\sim$0.4) during the main-shock occurrence. The Al-Ays lava-field is inferred to underlie a seismic volume trending NW-SE bounded on both sides by two NW-SE trending fault systems, dipping 40–50° opposite to each other within a proposed nascent rift setting.

1. Introduction

Southwestern Saudi Arabia except the Red Sea region is seismically inactive, though repeated basaltic eruptions here covered a vast expanse of volcanic fields, called the "Harrats" (figure 1). The harrats form the volcanic fields that are historically stable, which, experience periodic small swarms or sometimes a sizeable earthquake event. Table 1 provides a list of instrumentally recorded events since 1964 plus a well documented event that occurred in 1121 AD. Since 2007, recording of periodic small earthquake swarms in the area prompted the Saudi Geological Survey (SGS) to fix a network of broadband seismometers surrounding the volcanic field with real-time

---

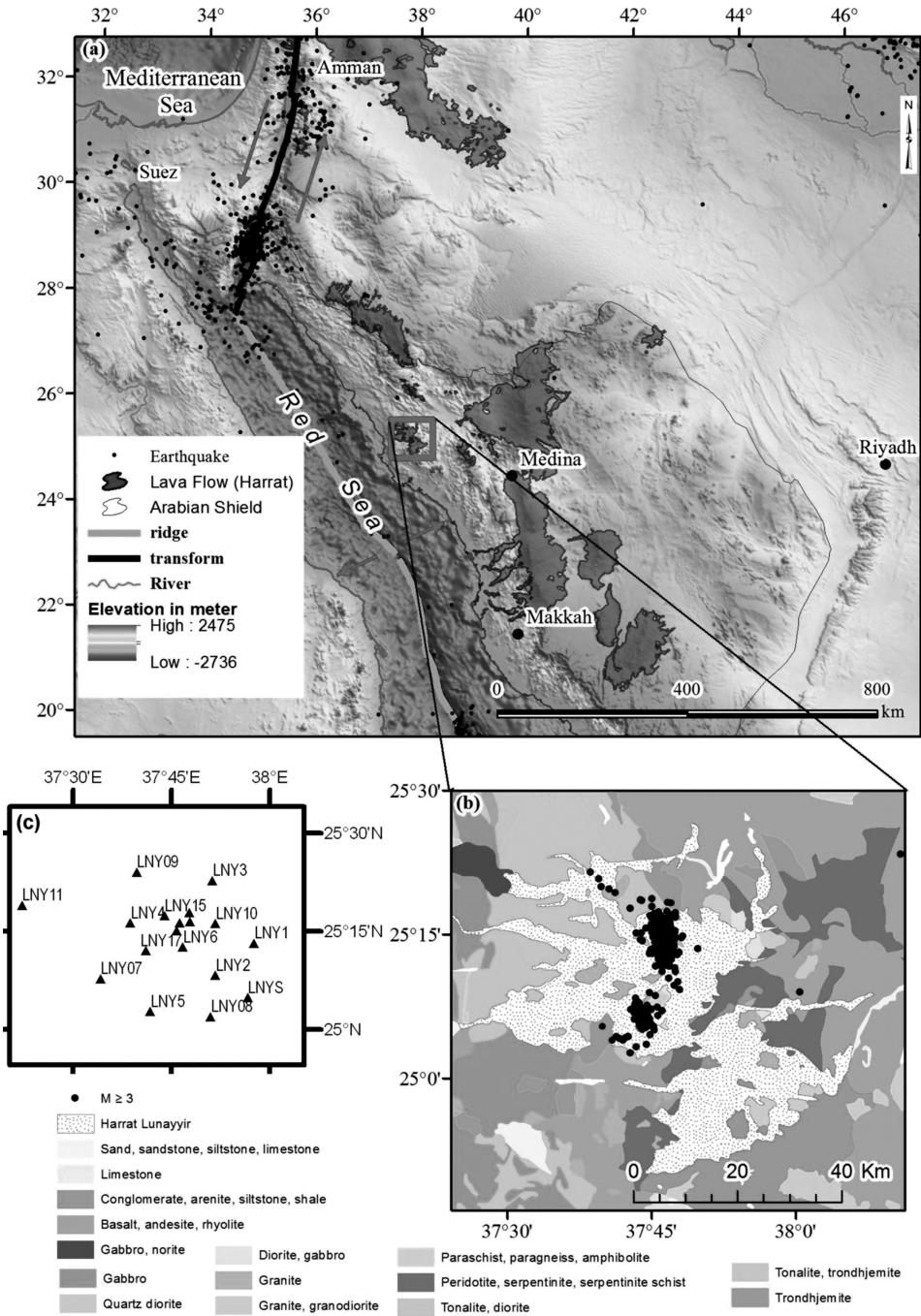*Corresponding author. Email: basabmukhopadhyay@yahoo.com

Figure 1. (a) Generalized location of the western Arabian Shield with Cenozoic volcanic provinces and the study area marked with box. (b) The blow up geological map of the Harrat Lunayyir with arc related rocks (plutonic + volcanic) of the study area with earthquake data of the swarm (M ≥ 3). (c) Seismic network that captures the swarm data in the study area.

Table 1. Earthquake statistics in the study area and its surroundings prior to 2009 Al-Ays earthquake swarm.

Year	Number of events	Magnitude
1121	1	6.8
1964	1	4.8
1979	1	4.7
1987	1	3.32
1988	1	5.1
1992	1	4.8
1993	1	3.4
1995	2	3.4–3.44
1996	3	3.09–3.5
1997	1	3.09
1998	2	3.05–3.34
1999	4	3.1–3.7
2000	18	3.34
2001	7	3.06–3.76
2002	2	3.04–3.43
2003	1	3.3
2004	13	3.08–4.12
2005	17	3.0–3.62
2007	11	3.02–4.22
2008	3	3.04–3.15

data capture and transmission through VSAT to its Earthquake and Volcano Center at Jeddah. The new network system thus established had captured the seismic data of an earthquake swarm containing 15,029 seismic events with magnitude $M \geq 0.01$ during the period from 15.05.2009 to 30.09.2010. The swarm, which culminated with a main shock of M 5.4 earthquake on 19 May 2009 (17 Hrs 34 Min 58 Sec, Mw 5.7, focal depth 7.81 km) caused very minor structural damage in the town of Al-Ays, but produced a worldwide interest due to the numerical strength of tremors within a relatively short time-span. The general degree of damage indicates a maximum predominant intensity of VI in Modified Mercalli Intensity scale (Al-Amri and Fnais 2009) around epicenter. A joint SGS-USGS study accompanied by geologic, geodetic and seismic surveys confirmed the volcanic nature of the swarm activity and registered some salient seismotectonic observations (Zahran et al. 2009; Pallister et al. 2010) that are summarized below:

- A 3-km-long NW-trending surface rupture appeared in the central part of the Harrat before 19 May 2009, during a time when maximum earthquake magnitudes exceeded M 4. The length of this rupture extended to 8 km with the M 5.4 earthquake on 19 May 2009 with 91 cm offset. The rupture opened 0.5 m and had an absolute motion of 0.9 m to N35°W with 63° plunge to the NE – a tensional offset consistent with that expected from an M 5.4 earthquake in a rift-shoulder setting.
- InSAR data showed about a meter of extension and uplift (as of July 2009) with the majority of deformation associated with the 19 May 2009 M5.4 earthquake. The InSAR-derived deformation field is best modelled by intrusion of a narrow (~ 2 m wide), 10-km-long dyke to shallow crustal levels.

- Tectonic models are offered that produced the Al-Ays swarm: (1) Stalled eruption or dyke intrusion (Zahran *et al.* 2009), (2) Rift-related extension recorded by dyke intrusion (Pallister *et al.* 2010), (3) Distant lithospheric flow away from the Red Sea trough beneath the Al-Ays (Ebinger and Blachew 2010) and (4) dyke intrusion and opening of volcanic rift inferred from InSAR measurements and elastic modelling (Baer and Hamiel 2010).

None of the above models investigate the dyke intrusion process and rift tectonics using the earthquake swarm data. Here our objectives are to investigate the proposed hypothesis on dyke intrusion and rifting during the Al-Ays swarm. This is undertaken both in terms of its distribution on surface map and sections, its seismotectonic characteristics, relationship between the formation of the swarm sequence with the pore pressure perturbation process by deploying the "*r–t* plot", mapping of spatio-temporal "b-value" and thereby detecting anomalies and finally to generate an empirical model combining all to explain the mechanics of the earthquake sequence.

2. Geology in and around Harrat Lunayyir

The western part of the Arabian Shield (figure 1a) is consisted of metamorphosed volcano-sedimentary Proterozoic sequences of older Baish, Bahah and Jeddah Groups (950–800 Ma) and younger Halaban (Hulayfah) and Al Ays groups (800–650 Ma) with arc-related plutonic rocks of diorite to tonalite composition (Al-Amri and Fnais 2009). The youngest Al Ays Group has an intrusive relationship with the former volcano-sedimentary sequences (Stoeser and Camp 1985; Johnson 2000). The basaltic lava fields (harrats) of Saudi Arabia, Cenozoic to Recent in age, are developed directly on the Precambrian Arabian Shield. The study area (inset in figure 1a), Harrat Lunayyir is characterized by Cenozoic basaltic flows placed along with arc-related plutonic rocks of diorite to tonalite composition (figure 1b) having imprints of several cycles of metamorphism and tectonism during Tertiary–Quaternary age (Al-Amri and Fnais 2009). Out of 21 eruptions recorded in the Arabian Peninsula during the past 1500 years (Camp *et al.* 1987), the intra plate volcanic eruption on Harrat Lunayyir about 1000 years ago is significant. It has experienced a series of volcanic eruptions that took place along related fissures and cinder cones forming a zone of N-S and NW-SE trends. Since Miocene, Lavas reached the ground surface through the prevailing deep crakes and fissures. Two sets of fault system have been identified in and around Harrat Lunayyir – (1) one set with NE-SW trend controlled mainly by older Precambrian faults that reactivated during the Tertiary age due to the opening of the Red Sea and ocean floor spreading and (2) other set with NW-SE direction that is responsible for rifting and opening of the Red Sea. The uplift and volcanism in the Arabian Shield including Harrat Lunayyir are generally assumed to be the result of hot, buoyant material in the upper mantle that may have eroded the base of the lithosphere (Camp and Roobol 1992). The low seismic velocities beneath the Arabian Shield and Red Sea at depths below 200 km are related to mantle upwelling and seafloor spreading (Al-Amri *et al.* 2008).

3. Earthquake data analysis

The 15,029 seismic records (see the seismic network in figure 1c) with M $\geq$ 0.01 recorded from the period 15.05.2009 to 30.09.2010 collected by SGS within the study

area (figure 1) are plotted on a topographic contour map with magnitude bins (figure 2). On map, the seismicity follows an eye-shaped pattern with larger earthquakes including the main-shock at its centre following the slope of NW-SE trending spar. The Log (cumulative number, N) – magnitude (M) curve (figure 3a) over the magnitude M ≥ 0.01 is not smooth and follows a straight-line segment only after M ≥ 1.01. Log N–M curve for the swarm data over M ≥ 1.01 is smooth (figure 3b) and clearly suggests that all earthquakes above magnitude 1.01 were detected as per the Gutenberg–Richter relationship and this value can be treated as magnitude (M_c) completeness. The catalogue is thus by and large complete above the threshold magnitude 1.01 within the specified time frame that has been used here for further analysis. The b-value calculated by regression method through Log N–M plot for 12,182 numbers of seismic events with M ≥ 1.01 is 0.96.

Earthquake swarms are sequences of earthquakes closely clustered in space and time, in which no single earthquake dominates in size (Scholz 2002) i.e. many earthquakes of the same size occurring in a small volume. Another typical feature of
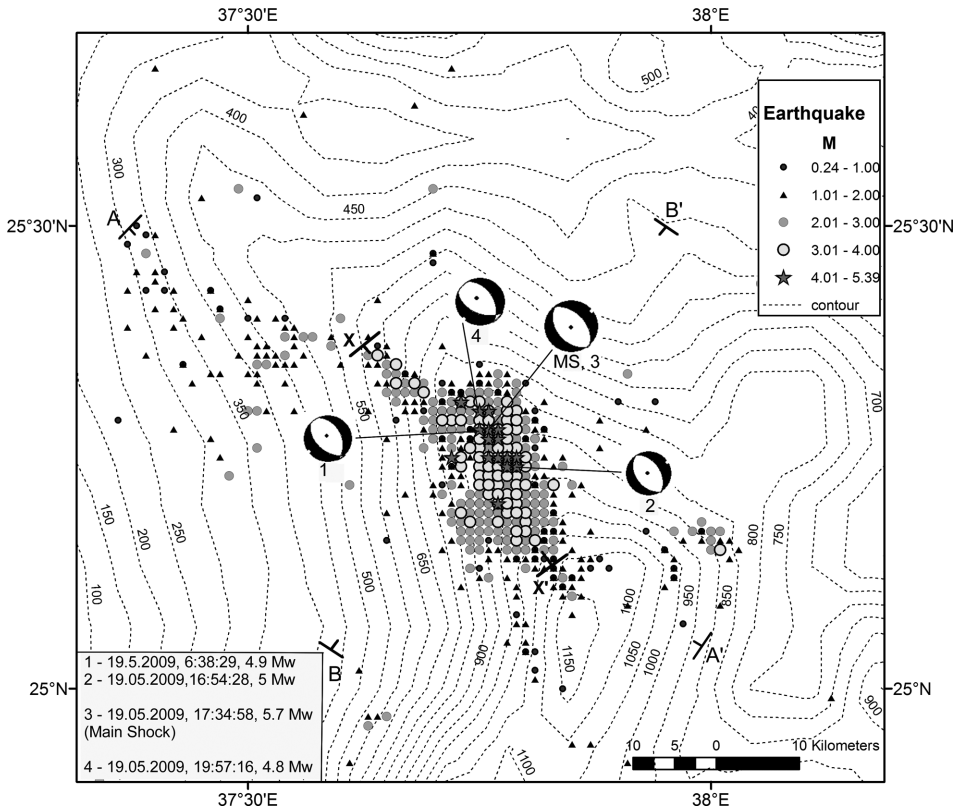

Figure 2. Microseismicity map for the town Al-Ays in SW Saudi Arabia. Local Station Earthquake data [Data Source: SGS] are plotted with magnitude in suitable bins. Notice the eye shaped seismic zone placed along a NW-SE trending spar. Four major earthquakes including the main shock with normal CMT solutions along fault planes trending NW-SE are plotted. The swarm mostly affected topographically elevated parts. Two bounding fault planes trending NW-SE dipping towards each other but not reaching the surface can be inferred from the earthquake volume. A–A', B–B' and X–X' are section lines.
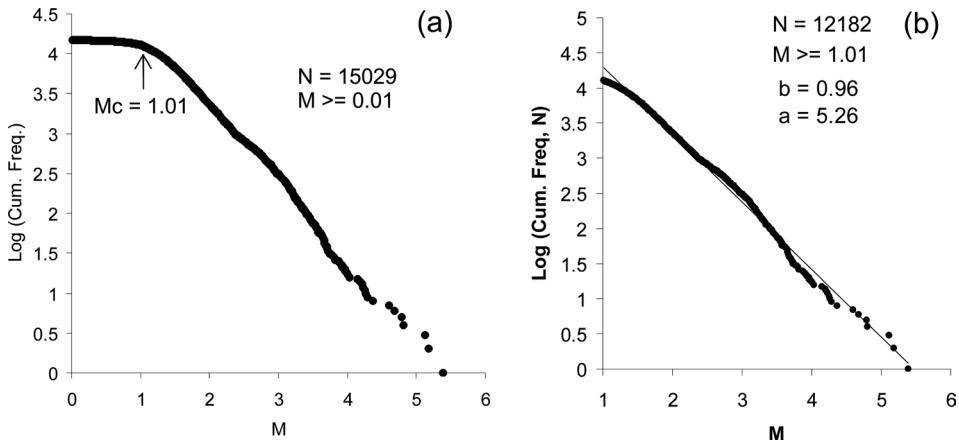
Figure 3. Frequency–magnitude relationships for: (a) 15,029 events of M ≥ 0.01. Notice that the catalogue is almost complete above the threshold magnitude 1.01 for respective time frames, (b) FMD plot for 12,182 earthquakes with M ≥ 1.01 and their respective "a" and "b" values.

the earthquake swarms is the relatively small magnitude differences between the main shock, the second largest event and the subsequent ones within a swarm sub-sequence and consequently, within the whole swarm. According to the information available regarding swarm, the magnitude differences between the largest and the second largest can be assumed to be smaller than 0.45 (Grunthal *et al.* 1990). In this case though a main-shock is identified as earthquake of M 5.4 (19.05.2009, 17 Hrs: 34 Min: 58 Sec, focal depth 7.81 km), the subsequent close by higher shocks are registered with magnitude M 5.18 (19.05.2009, 16Hrs: 54Min: 28 Sec, focal depth 9.88 km) and M 5.12 (27.08.2009, 20 Hrs: 22 Min: 27 Sec, focal depth 1.77km). Thus the difference in magnitude is only 0.22 and 0.28 respectively which is within limit of 0.45 as stated by Grunthal *et al.* (1990). Thus the sequence can be assigned to be a swarm like sequence occurring in a small volume.

Two broad section lines, one longitudinal (A–A') and another cross section (B–B') (figure 2) are drawn to decipher the shape of the seismic volume (figure 4). The sections indicate an elongated funnel shaped seismic zone with main-shock occurring at its centre. Majority of earthquakes are shallow crustal coming from 0 to 15 km depth. The narrow, vertical and linear zone of seismicity present at a depth higher than 20 km in both the sections indicate possible area/zone of dyke intrusion. The central position of the dyke intrusion is inferred to be a point with Latitude 25.22°, Longitude 37.82°, at a depth ~20 km from these sections. This point is taken as the point from which the fluid diffusion process has been initiated and is used as the reference point to construct the r–t plot. The CMT data of four major shocks collected from HRVD website are plotted on the map as beach ball circles (figure 2, table 2). The data indicates that the main shock and three other larger shocks are originated from fault planes trending NW-SE dipping 40°–50° on either side by the process of normal/gravity movement. The compression axis is near vertical with high plunge (>70°) whereas the tensional axis is sub-horizontal (2°–3°) trending NE-SW in conformity with the opening trend of the Red Sea. The 14 numbers of composite fault plane solutions including the main-shock constructed by Al-Amri and Fnais (2009) indicate trans-tensional tectonic scenario perpendicular to major structural

trend NW-SE, which correlate well with the field measurements of ground cracks
and fissures accompanied with the mainshock.

The depth–time plot (figure 5) of the earthquakes indicates that earthquakes are
originating in the study area roughly from two depth bands, 5–10 km and 15–20 km
respectively with a relatively less seismic zone in between. Initially i.e. from 0 to 125
hrs time frame, earthquakes are mainly concentrated along 5–12 km depth band
with occurrence of the major shock of M 5.4 on 19 May 2009 (17 Hrs 34 Min 58 Sec,
Mw 5.7, focal depth 7.81 km). The occurrence of further shallow crustal earthquake
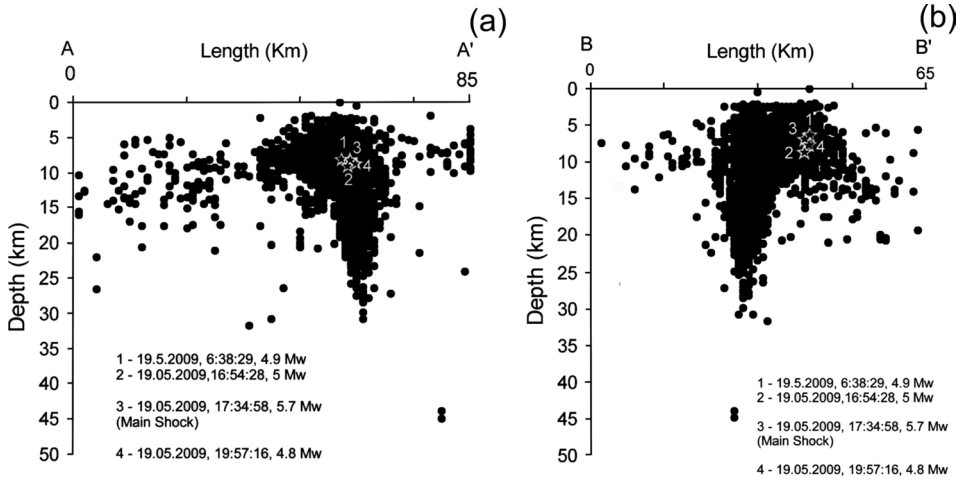

Figure 4. Vertical sections representing the seismogenic volumes. (a) Longitudinal section
along A–A' and (b) Cross section along B–B' (Figure 2 for section locations). Both sections
exhibit a funnel shaped seismic volume. Fluid diffusion initiates from the injection point
inferred at Lat. 25.22°N and Long. 37.82°E.
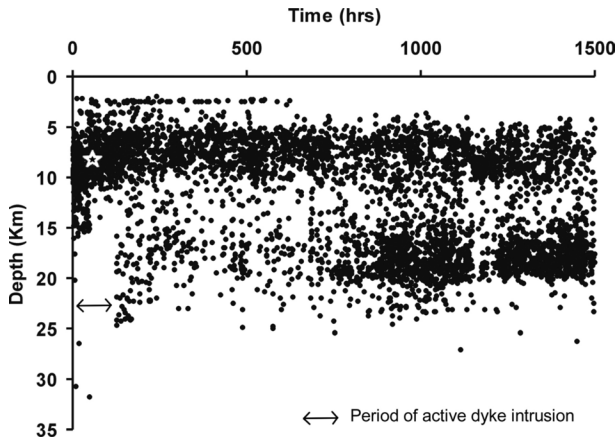

Figure 5. Depth–time section of the earthquakes (M $\geq$ 1.01) in the swarm showing two depth
bands 5–10 km and 15–20 km with a less pronounced seismic zone in between. Absence of
earthquakes in the depth band 16–25 km, initially within the period 0–125 hours, is
conspicuous, and probably suggests for the time of active dyke intrusion. Star is the time of
main shock occurrence.

with depth bands 0–5 km is small in number. After the occurrence of the major shock the seismicity migrated deeper and occupied the crustal space from 15 to 20 km with concurrent occurrence of seismicity within 5–10 km band too. We infer that the first 0–125 hrs time span (i.e. 15/5/2009 0 Hrs: 2 Min: 42 Sec to 20/5/2009 5 Hrs: 14 Min: 8 Sec) is the activity time of the dyke intrusion after which its activity diminishes. The pore-pressure perturbation due to this dyke intrusion to generate swarm sequence is discussed in the next section.

4. Pore presssue perturbation

Pore pressure diffusion as a triggering mechanism has been proposed for many case studies; e.g. fluid-injection induced earthquakes (e.g. Shapiro *et al.* 1997; Rothert and Shapiro 2003; Shapiro *et al.* 2003; Antonioli *et al.* 2005), reservoir induced (e.g. Ferreira *et al.* 1995); intraplate earthquake swarms (e.g. Parotidis *et al.* 2003) etc. We also assume that pore pressure diffusion is a possible mechanism for triggering swarm activity in our study area. The relationship between the swarm sequence and its causative pore pressure perturbation is studied by a process called the "*r–t* plot" what is based on the diffusion equation for a point pore pressure source in a homogeneous and isotropic fluid saturated poro-elastic medium having specific hydraulic properties. Shapiro *et al.* (1997, 2002) predict that fluid flow may trigger an earthquake at a location "*r*", at any time "*t*", after the pressure perturbation. The distance "*r*" of the propagating pore pressure front from the injection point (that acts as a source with $t = 0$), with $r = \sqrt{(4\pi Dt)}$, is estimated as a function of time (*t*). The equation actually defines the enveloping parabola in the *r–t* plot with variable hydraulic diffusivity (D) values, where, seismicity points should lie below the modelled parabolic curve. The "D" is scalar; whose value depends on permeability (k), uniaxial specific storage coefficient (S) and viscosity of the fluid (μ) by the equation $D = k/(\mu S)$ (Kuempel 1991, Wang 2000). On the contrary, if the earthquake triggering occurs shortly after the pore pressure perturbations (Noir *et al.* 1997), we should observe a narrow cluster of seismicity along the line of the modelled parabola in the *r–t* plot with variable scalar D values. The D-value in the earth's crust usually ranges between 0.1 and 10 m^2/s (Shapiro *et al.* 1999) but can reach to 90 m^2/s (Antonioli *et al.* 2005) but there is no upper limit. In this scheme the *r–t* plot basically represents spatial distance "r" of an individual event from the injection point as a function of time "*t*". An unambiguously defined injection point source, which corresponds to the origin of the graph at time 0, is therefore a pre-requisite for calculation purpose (Shapiro *et al.* 1997). The injection point from which the fluid diffusion starts in this case is with Latitude 25.22°, Longitude 37.82°, depth $\sim$20 km identified from the sections (figure 4) from where the fluid actually begins to propagate (for further explanation on injection point, refer Shapiro *et al.* 1997, 2002, 2003) and is used as initial reference point to construct the *r–t* plot. This point is determined from the vertical projection of the points that creates a linear disposition of earthquake epicenters in figure 4. The earthquake points in the *r–t* plot with modelled diffusivity value D of 0.1 m^2/s lie below the modelled parabolic curve (figure 6), where, the swarm relates to the diffusion of pore pressure in a poro-elastic fluid saturated medium. The pore-pressure perturbations that generate earthquake swarm in divergent pull-apart basins are initiated by magmatic dyke intrusion from mantle source (also refer Mukhopadhyay *et al.* 2010, 2011). A very high pore pressure activity with low diffusivity along narrow zone of volcanic dyke intrusion
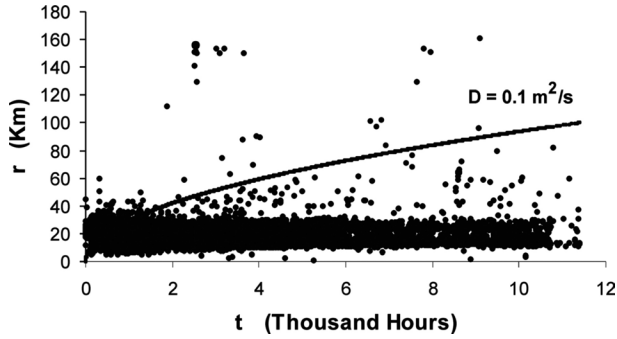
Figure 6. The *r–t* plot corresponding to 12,182 earthquakes contained in the Al-Ays swarm (M ≥ 1.01) with modelled parabolic envelope of diffusivity (D = 0.1 m²/s). Note the pore pressure protuberance in respect of time as generated due to dyke intrusion.

with depths from 15 to 20 km can be inferred. The low diffusivity is depicting a fractured medium generated due to past intrusions of dykes through which the pore pressure perturbation took place. The existence of mantle plume beneath the western part of the Arabian plate including Harrat Lunayyir has been recognized by several studies (Benoti *et al.* 2003, Daradich *et al.* 2003, Julia *et al.* 2003, Al-Damegh *et al.* 2005) with surface expression of the plume-related ocean-island basalt volcanism (Moufti and Hashad 2005). Pronounced degassing of the CO_2 dominate upper mantle is probably the source of the H_2O plus CO_2 dominated fluid (cf. Plenefisch and Klinge 2003 for discussion).

5. Variations in spatio-temporal b-values

The earthquake size distribution (frequency-magnitude distribution, FMD) follows the well-known power law, designated as b-value, which is commonly used to designate the relative occurrences of large and small earthquake events (Schorlem-mer *et al.* 2005). The b-value in the present study has been estimated by maximum-likelihood method (Bender 1983), $b = log_e/(M–M_{min})$, where M denotes the mean magnitude and M_{min} the minimum magnitude of the given sample. Both spatial and temporal b-values are calculated. The spatial b-values along a vertical section (along X–X' line of figure 2) are computed by a volume of 5 km × 5 Km × 5 km on both side of the section line with 2.5 km overlap both along strike and dip of the vertical section. These b values are plotted on the section and are manually contoured (figure 7). The higher b-value (>1.3) is concentrated along a low volume with length 10 km and height 5 km immediately below the zone where main-shock and other larger earthquakes occurred. This anomalous b value zone is embedded with in a background of normal b (b ≤ 1.) value. Such smaller anomalous volume due to volcanic activity in a crust embedded with normal b-value have been reported below the volcanoes in several other studies: Off-Ito volcano (Wyss *et al.* 1997), Long Valley and Mammoth Mountain (Wiemer *et al.* 1998), Montserrat (Power *et al.* 1998), Etna (Murru *et al.* 1999), Katmai (Jolly and McNutt 1999) and East rift zone of Kilauea (Wyss *et al.* 2001).

A slight increase in b-value (∼ .0) just above this anomalous volume is typical of swarms in intra-plate settings (Plenefisch and Klinge 2003) which give the main-shock, allied larger earthquakes and other shocks. Similar condition with b-values
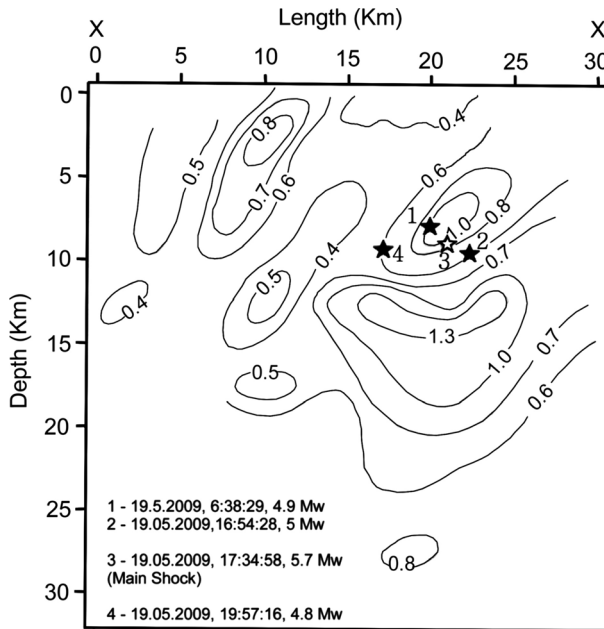
Figure 7. Contoured b-value along the section X–X' of Figure 2. Anomalously high b-values (>1.3) are found beneath the larger earthquakes while the seismic cluster is embedded in a low b-value volume.

(up to 1.3 ± 0.1) associated with the Hebgen Lake fault zone west of the Yellowstone caldera was related to the transport of magmatic fluids out of the Yellowstone volcanic system (Farrell *et al.* 2009). Other factors causing this high b-value may be the presence of hot fluids in geothermal systems or extensive cracking during earthquakes or acquired during past eruptions (Wiemer and Wyss 2002).

The temporal distribution of "earthquake numbers" and "b-values with time" calculated on the earthquakes on 24 hours basis are plotted (figure 8). The diagram (figure 8a) indicates ups and down in the earthquake numbers during first 3500 hours (∼146 days) period. From the periodic variation of the earthquake numbers we speculate impulsive nature of the shocks and possible 10 such major pulses number P-1 to P-10, though many other minor pulses within this time exist. Similarly, the temporal b-values calculated on the basis of 24 hours by maximum likelihood method and are plotted. The values disposed as a parabolic curve (figure 8b). The curve indicates that the b-value increases rapidly (ranges from 0.24 to 1.16) in between 0 and 1608 hrs (i.e. first 67 days) and then stabilizes around an average value 0.88 thereafter. It is known the value "b" acts as a "stressmeter" in earth crust and depends inversely on the applied differential stress and tectonic character of the region (Hatzidimitriou *et al.* 1985, Tsapanos 1990). Initial high shear stress within the system during the generation of main-shock is reflected by a very low b-value (∼0.4). Subsequently with the release of energy as the effective stress decreases the b-value started rising. The b-value stabilizes as and when the effective stress is neither increasing or decreasing and getting stabilize in congruence with the regional stress field.
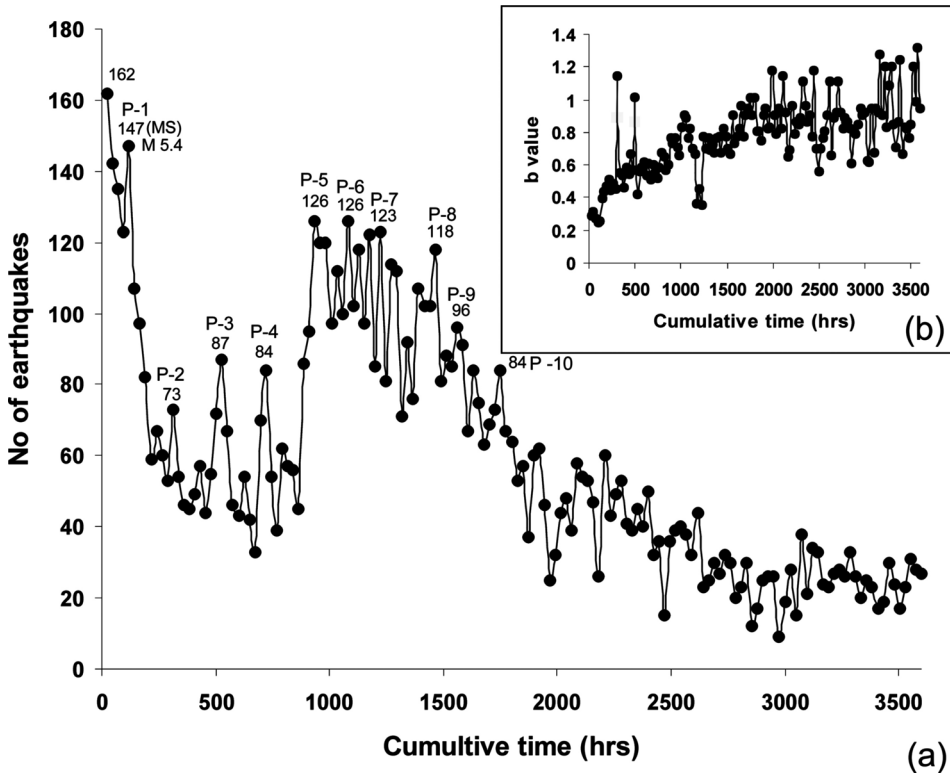
Figure 8. Plot of the number of earthquakes with cumulative time indicates: (a) pulsating nature for the earthquake generation with ten or more such possible pulses. (b) The temporal b-value variation follows a parabolic equation with an initial rapid increase but stables down as the time progresses.

6. The swarm model

6.1. *The existing models explaining swarm sequences*

Several mechanisms have been proposed for the earthquake swarm generation and are succinctly summarized in Kurz *et al.* 2003 and 2004 and other related publications. The models are conceptualized in a way that they are complementing one another.

The initial model given by Mogi (1963) suggested that in highly fractured regions, stress concentrations around fractures promote failure already under small stresses without the occurrence of large rupture surfaces. This small ruptures generate swarm type earthquake sequence.

The dilatancy–diffusion model (Nur 1972) assumes that dilatancy occurs within the stressed volume surrounding an impending rupture zone. In active fault zones, dilatancy (increase in pore space by shearing) is created by volume expansion through opening and widening of cracks prior to rupture and production of extension veins and grain-boundary sliding by induced tectonic stresses. Dilated spaces are generally filled with either water or rock fluids. Increase in pore pressure along fault zone results into decrease in effective stress and promote small slips along the fault planes generate swarms.

Later models are mostly based on the Mohr–Coulomb failure theory in its effective stress formulation. Hill (1977) proposed a model for volcanic regions or rifted areas with volcanic connotation. The model assumes a system of magma-filled dykes interconnected by stress-field oriented fractures may rupture under certain pore pressure conditions in the dyke. It also stated that magma injection in rifted areas commonly invokes the injection of shallow, vertical, en-echelon dykes extending along a narrow rift zone. The injection accounts swarms with initial strike slip motion during opening phase followed by the collapse of closely spaced inner rift wall with earthquakes of normal fault source mechanism. Furthermore, material and stress heterogeneity can be attributed to an increase in fluid pressure within a system of dykes under a regional deviatoric stress field. Shear failures occur along oblique fault planes connecting adjacent tips of offset dikes when a critical combination of the fluid pressure in the dykes and the regional stress difference are achieved.

Swarm-like sequences could also be created by fluid flow from localized high pressure compartments when fractures are controlled by increasing permeability (Yamashita 1999). The spatio-temporal variation of rupture activity is modelled assuming that the fluid migrates along a narrow porous fault zone in a semi-infinite elastic medium. As faults slip, pores are created and the Coulomb failure criterion introduces mechanical coupling between faults slip and pore fluid. The fluid flows from a localized high-pressure fluid compartment in the fault with the onset of earthquake rupture. The duration of the earthquake sequence is assumed to be considerably shorter than the recurrence period of characteristic events on the fault and rupture process is significantly dependent on the rate of pore creation. If the rate is large enough, a foreshock–mainshock sequence is never observed; the rupture sequences generate earthquake swarms. Such sequences generally start and end gradually with no single event dominating in the sequence. The model shows that a foreshock–mainshock sequence is only observed if the critical slip distance for pore creation is infinite, i.e. no pores are created by any slip in the model and the whole fault is moving.

Another model proposed by Tzschichholz and Wangen (1999) introduces hydraulic fracturing of a porous material in presence of high fluid pressure. It says that crack start to move after the onset of fluid injection. This process decreases the strength and the hydraulic pressure within the material. The crack propagation comes to an end after some time when a critical cohesion and hydraulic pressure is reached. The fluctuation in fluid injection induces more cracks initially but frequency of crack propagation becomes larger as the time goes by. This spatio-temporal fracture behaviour generated by the micro-mechanical hydraulic fracturing induces the swarm sequence. The micromechanical approach of Tzschichholz and Wangen (1999) also complements the results of Yamashita (1999). Both these models do not introduce the range of magnitude distribution within the clustered events.

Within this premise, a model combining the hydro fracturing with respect to periodic pore pressure variations and temperature changes has been proposed (Kurz *et al.*, 2004) for swarm generation in Vogtland/Western Bohemia earthquake swarm region.

6.2. *Proposed model for the Al-Ays earthquake swarm*

Our proposed model is a combination of models given by Hill (1977) and Yamashita (1999). From the compilation of the evidences generated so far like earthquake distribution on plan and sections, fault plane solution data, depth–time plot, pore

pressure perturbation by *r–t* plot, spatial and temporal b-value distribution for the Al-Ays swarm activity, we infer a dyke intrusion model within the crust fits well to explain the seismic sequence. A schematic model to narrate this is presented (figure 9). From the plan (figure 2) and depth sections (figure 4) we infer a funnel shaped NW-SE trending seismic volume bounded on both sides by two NW-SE trending fault systems dipping 40°–50° opposite to each other in a rift environment and exposed to the surface. From the b-value in section (figure 7) we infer that dyke intrusion probably took place along a narrow zone with width 10–15 km from the active mantle plume at a depth of $\sim$20 km below surface. Similar dyke intrusion phase but without seismicity, has also been recorded in weakly extended Natron rift in Tanzania (Calais *et al.* 2008). This dyke intrusion induces a pore pressure perturbation with fluids generated from pronounced degassing of the CO_2 dominate upper mantle (as inferred by Plenefisch and Klinge 2003 in other place). H_2O part of the fluid may be a product of dehydration of crustal material during metamorphism. However, no gas emissions or explosions were reported at Lunayyir (Pallister *et al.* 2010). The high b-value around the dyke intrusion zone (b $>$ 1.3) also made its contribution of fluids to ruptures and the high rate in pore creation by fault slips as per swarm generation mechanism proposed by Yamashita (1999).

We assume that a rift basin is in its nascent state that has developed in the study area due to tensile stresses from far field plate motions. The rift is parallel to the Red
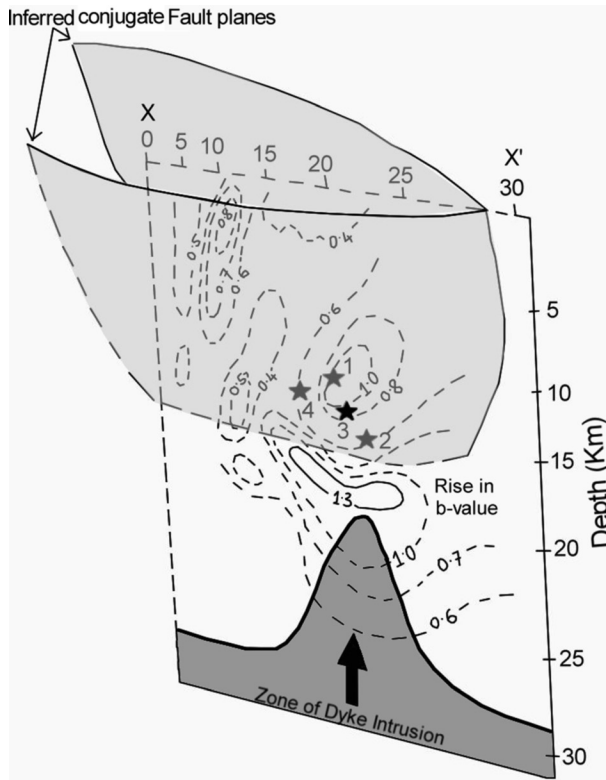

Figure 9. A conceptual model for dyke intrusion and generation of earthquakes, with clear interaction of two fault planes.

Sea and evidences of its presence have been documented by Baer and Hamiel (2010) from InSAR measurements and elastic modelling. Further, body and surface wave tomography (Nyblade *et al.* 2006) suggest that the mantle lithosphere beneath the Arabian Shield has been thermally modified and that there is an abrupt change in lithospheric structure across the Shield–Platform boundary, which is also observed in the regional gravity data (Hansen *et al.* 2007). The rapid lithospheric thinning near the Red Sea rift likely channelize hot asthenospheric flow (Daradich *et al.* 2003; Hansen *et al.* 2006) and thermal modification of tectonic environments. The thermal modification has promoted the dyke intrusion from the upwelling mantle that has uplifted the crust by a meter in the earth surface as recorded from the InSAR data analysis (Zahran *et al.* 2009) but without volcanic eruption in contrast to the adjacent Afar rift in Ethiopia with minor volcanic eruption (Sigmundsson 2006). Due to vertical pressure exerted by dyke intrusion in the crust at a depth of ~ 20 km, two new shear surfaces/faults trending NW-SE dipping opposite to each other have formed in the rift to compensate the vertical push of dyke as per the model of Hill (1977) and Yamashita (1999). During this time, the compression axis (σ_1) is near vertical (see the P axis plunge which is $> 72°$ in table 2) whereas the extensional (σ_3) axis is sub-horizontal (see T axis plunge which is $2°$–$3°$ in table 2). The junction between the faults planes is the intermediate axis σ_2. As per Hills model, shear failures along these oblique fault planes occur when a critical combination of the fluid pressure in the dikes and the regional stress difference $\sigma_1 - \sigma_3$ is attained. The earthquake swarm is formed if the regional tectonic stress difference $\sigma_1 - \sigma_3$ remain constant or slightly variable while the fluid pressure in the system of dykes gradually increases. This is precisely the case here. The earthquakes of higher magnitudes originated just above the junction of the inferred faults (summarized from CMT data) as a process of dissemination of the ambient stress generated down below by dyke intrusion. The strain caused by dyke intrusion process is released in the form of numerous earthquakes with increase of fluid pressure. The dyke intrusion process though started long back prior to the generation of this seismic sequence lasted for a very small amount of time (with first 125 hours, figure 5) during the recording of this seismic episode where no earthquakes are noticed at a depth 20 km and below due to presence of hot fluids. This hot fluid caused pore pressure perturbations as indicated by the *r–t* plot (figure 6) with very low diffusivity. The effect of intrusion subsides or becoming ineffective in a later phase, the crustal volume surrounding the dyke intrusion within depth between 17 and 25km was filled with numerous earthquakes characterized by small length rupture zones. Furthermore, if we consult the "Magma injection model" of Hill's (Hill 1977) in rifted areas which commonly invokes the injection of shallow, vertical, en-echelon dykes extending along a narrow rift zone, this injection accounts initial strike slip motion along the fault planes followed by the collapse of closely spaced inner rift wall with earthquakes of normal fault source mechanism. The same is corroborated by other studies (Bergmann and Solomon 1990, Elsworth and Voigt 1995) including our own study in the South Andaman Sea (Mukhopadhyay *et al.* 2010). In this Al Ays swarm sequence; we only have normal earthquakes (table 2). This is clearly suggestive of the waning phase for the intrusion that is marked by collapsing of the rift wall. This evidence is precisely corroborated the vertical orientation of compression axis (σ_1) which only promote gravity faulting compensating the initial uplift of the crust by 1m on the surface. This is again the reason why there was no volcanic extrusion in this zone. However, this does not obviate the likelihood of a future eruption or large earthquake in the Al-Ays volcanic

Table 2. CMT solution parameters for major earthquakes contained in the Al-Ays earthquake swarm (source HRV).

Date	Time (Hr:Mn:Sec)	Lat	Long	Depth (Km)	M	Mw	Plane1 Azimuth	Plane1 Dip	Plane1 Rake	Plane2 Azimuth	Plane2 Dip	Plane2 Rake	P Azimuth	P Plunge	T Azimuth	T Plunge	Scalar moment (dyne-cm)	Solution
19/5/2009	6:38:29	25.28	37.75	7.76	4.81	4.9	337	43	−73	134	49	−105	341	78	235	3	2.45×10^{23}	Normal
19/5/2009	16:54:28	25.27	37.77	9.88	5.18	5.00	145	42	−94	329	48	−87	278	86	57	3	4.2×10^{23}	Normal
19/5/2009	17:34:58	25.28	37.76	7.81	5.39	5.70 (MS)	143	42	−88	320	48	−92	208	87	51	3	3.97×10^{24}	Normal
19/5/2009	19:57:16	25.30	37.75	8.68	4.79	4.80	330	46	−64	115	50	−114	318	72	222	2	1.91×10^{23}	Normal

zone as the ambient stress due to dyke intrusion still exists. As the rupture planes of the larger earthquakes reach the ground level (Zahran *et al.* 2009, Pallister *et al.* 2010), these planes may act as an easier conduit for future volcanic activity.

7. Conclusions

The 2009 earthquake swarms of Al-Ays in Harrat Lunayyir with 12,182 numbers of seismic events with $M \geq 1.01$ forms an elongated funnel shaped NW-SE trending seismic zone with main-shock and larger shocks occurring at its centre. Majority of earthquakes are of shallow crustal origin that came from two depth bands (5–10 and 15–20 km) with a relatively less seismic zone in between. We propose a dyke intrusion model as a proposed mechanism for this swarm based on the supporting data, r–t plot and inference model. An incipient status of dyke intrusion is suggested by modelling results for the 2009 Al-Ays earthquake swarm. Dyke intrusion that primarily started had a peak period during the initial time span of 5 days (15/5/2009 to 20/5/2009) of recording the events, after which its activity diminishes. The r–t plot of this swarm with modelled low diffusivity (D = 0.01) relates the diffusion of pore pressure to seismic sequence in a fractured poro-elastic fluid saturated medium. The high spatial b-value (>1.3) along the section reflects the zone (length 10 km and height 5 km) of dyke intrusion at a depth of ~ 20 km from surface. The main-shock and other larger earthquakes are originated on a moderate b-value zone (~ 1.0) top of the anomalous b-value zone (>1.3) created by dyke intrusion. Temporal b-value analysis indicate a very low b-value (~ 0.4) during the main-shock occurrence and stabilizes to an average 0.88 as and when the effective stress is neither increasing nor decreasing. From our proposed model we infer a seismic volume trending NW-SE bounded on both sides by two NW-SE trending fault systems dipping 40–50° opposite to each other to form a nascent rift. The high b-value around the dyke intrusion zone (b > 1.3) also made its contribution of fluids to ruptures and the high rate in pore creation by fault slips as per swarm generation mechanism proposed by Yamashita (1999). At this stage we cannot rule out the likelihood of a future swarm accompanied by and/or eruption as the ambient stress due to dyke intrusion still exists and there is a provision of renewed dyke intrusion.

References

AL-AMRI, A. and FNAIS, M., 2009, Seismo-Volcanic investigation of 2009 swarms at Harrat Lunayyir (Ash Shaqah), Western Saudi Arabia. *International Journal of Earth Science and Engineering,* Oct. issue, pp. 1–18.

AL-AMRI, A., RODGERS, A. and AL-KHALIFAH, T., 2008, Improving the level of seismic hazard parameter in Saudi Arabia using earthquake location. *Arabian Journal of Geosciences,* **1**, pp. 1–15.

AL-DAMEGH, K., SANDVOL, E. and BARAZANGI, M., 2005, Crustal structure of the Arabian plate: new constraints from the analysis of teleseismic receiver functions. *Earth and Planetary Science Letters*, **231**, pp. 177–196.

ANTONIOLI, A., PICCININI, D., CHIARALUCE, L. and COCCO, M., 2005, Fluid flow and seismicity pattern: evidence from the 1997 Umbria-Marche (central Italy) seismic sequence. *Geophysical Research Letters*, **32**, p. L10311.

BAER, G., and HAMIEL, Y., 2010, Form and growth of an embryonic continental rift: InSAR observations and modelling of the 2009 western Arabia rifting episode. *Geophysical Journal International*, **182**, pp. 155–167.

BENDER, B., 1983, Maximum likelihood estimation of b values for magnitude grouped data. *Bulletin of the Seismological Society of America*, **73**, pp. 831–851.

BENOTI, M.H., NYBLADE, A.A., VANDECAR, J.C. and GURROLA, H., 2003, Upper mantle P wave velocity structure and transition zone thickness beneath the Arabian Shield. *Geophysical Research Letters*, **30**, pp. 1–4.

BERGMANN, E.A. and SOLOMON, S.C., 1990, Earthquake swarms on the Mid Atlantic Ridge: products of magmatic or extensional tectonics? *Journal of Geophysical Research*, **95**, pp. 4943–4965.

CALAIS, E., D'OREYE, N., ALBARIC, J., DESCHAMPS, A., DELVAUX, D., DÉVERCHÈRE, J., EBINGER, C., FERDINAND, R.W., KERVYN, F., MACHEYEKI, A.S., OYEN, A., PERROT, J., SARIA, E., SMETS, B.D., SARAH STAMPS, D.S. and WAUTHIER, C., 2008, Strain accommodation by slow slip and dyking in a youthful continental rift, East Africa. *Nature*, **456**, pp. 783–788.

CAMP, V.E. and ROOBOL, M.J., 1992, Upwelling asthenosphere beneath western Arabia and its regional implications. *Journal of Geophysical Research*, **97**, pp. 15255–15271.

CAMP, V.E., HOOPER, P.R., ROOBOL, M.J. and WHITE, D.L., 1987, The Madinah eruption, Saudi Arabia: magma mixing and simultaneous extrusion of three basaltic chemical types. *Bulletin of Volcanology*, **49**, pp. 489–508.

DARADICH, A., MITROVICA, J.X., PYSKLYWEC, R.N., WILLETT, S.D. and FORTE, A.M., 2003, Mantle flow, dynamic topography, and rift-flank uplift of Arabia. *Geology*, **31**, pp. 901–904.

EBINGER, C. and BLACHEW, M., 2010, Active passive margins. *Nature Geoscience*, **3**, pp. 670–671.

ELSWORTH, D. and VOIGT, B., 1995, Dike intrusion as a trigger for large earthquakes and the failure of volcano flanks. *Journal of Geophysical Research*, **100**, pp. 6005–6024.

FARRELL, J., HUSEN, S. and SMITH, R.B., 2009, Earthquake swarm and b-value characterization of the Yellowstone volcano-tectonic system. *Journal of Volcanology and Geothermal Research*, **188**, pp. 260–276.

FERREIRA, J.M., OLIVEIRA, R.T., ASSUMPCAO, M., MOREIRA, J.A.M., PEARCE, R.G. and TAKEYA, M.K., 1995, Correlation of seismicity and water level in the Acu Reservoir; an example from Northeast Brazil. *Bulletin of the Seismological Society of America*, **85**, pp. 1483–1489.

GRUNTHAL, G., SCHENK, V., ZEMAN, A. and SCHENKOVA, Z., 1990, Seismotectonic model for the earthquake swarm of 1985–1986 in the Vogtland/West Bohemia focal area. *Tectonophysics*, **174**, pp. 369–383.

HANSEN, S., SCHWARTZ, S., AL-AMRI, A. and RODGERS, A., 2006, Combined plate motion and density driven flow in the asthenosphere beneath Saudi Arabia: evidence from shear-wave splitting and seismic anisotropy. *Geology*, **34**, pp. 869–872.

HANSEN, S., RODGERS, A., SCHWARTZ, S. and AL-AMRI, A., 2007, Imaging ruptured lithosphere beneath the Red Sea and Arabian Peninsula. *Earth and Planetary Science Letters*, **259**, pp. 256–265.

HATZIDIMITRIOU, P., MOUNTRAKIS, D.P. and PAPAZACHOS, B., 1985, The seismic parameter b of the frequency-magnitude relation and its association with the geological zones in the area of Greece. *Tectonophysics*, **120**, pp. 141–151.

HILL, D.P., 1977, A model of earthquake swarms. *Journal of Geophysical Research*, **82**, pp. 1347–1352.

JOLLY, A.D. and MCNUTT, S.R., 1999, Seismicity at the volcanoes of Katmai National Park, Alaska; July 1995–December 1997. *Journal of Volcanology and Geothermal Research*, **93**, pp. 173–190.

JOHNSON, P.R., 2000, Proterozoic geology of Saudi Arabia: current concepts and issues. Contribution to a workshop on the geology of the Arabian Peninsula, 6th meeting of the Saudi Society for Earth Science, King Abdulaziz City for Science and Technology, Riyadh, Saudi Arabia. p. 32.

JULIA, J., AMMON, C. and HERRMANN, R., 2003, Lithosphere structure of the Arabian Shield from the joint inversion of receiver functions and surface-wave group velocities. *Tectonophysics*, **371**, pp. 1–21.

KUEMPEL, H., 1991, Poroelasticity: Parameters reviewed. *Geophysical Journal of International*, **105**, pp. 783–799.

KURZ, J.H., JAHR, T. and JENTZSCH, G., 2003, Geodynamic modelling of the recent stress and strain field in the Vogtland swarm earthquake area using the finite-element-method. *Journal of Geodynamics*, **35**, pp. 247–258.

KURZ, J.H., JAHR, T. and JENTZSCH, G., 2004, Earthquake swarm examples and a look at the generation mechanism of the Vogtland/Western Bohemia earthquake swarms. *Physics of Earth and Planetary Interiors*, **142**, pp. 75–88.

MOGI, K., 1963, Some discussions on aftershocks, foreshocks and earthquake swarms – the fracture of semi-infinite body caused by inner stress origin and its relation to earthquake phenomena. *Bulletin of Earthquake Research Institute, University of Tokyo*, **41**, pp. 615–658.

MOUFTI, M.R.H. and HASHAD, M.H., 2005, Volcanic hazards assessment of Saudi Arabian Harrats: geochemical and isotopic studies of selected areas of active Makkah-Madinah-Nafud (MMN) volcanic rocks. Final Project Report (LGP-5-27), King Abdlaziz City for Science and Technology, Riyadh, Saudi Arabia.

MUKHOPADHYAY, B., ACHARYYA, A., MUKHOPADHYAY, M. and DASGUPTA, S., 2010, Relationship between earthquake swarm, rifting history, magmatism and pore pressure diffusion – an example from South Andaman Sea, India. *Journal of Geological Society of India*, **76**, pp. 164–170.

MUKHOPADHYAY, B., MUKHOPADHYAY, M. and DASGUPTA, S., 2011, Seismic Clusters and their Characteristics at the Arabian Sea Triple Junction: Supportive Evidences for Plate Margin Deformations. *Journal of Geological Society of India*, **78**, pp. 131–146.

MURRU, M., MONTUORI, C., WYSS, M. and PRIVITERA, E., 1999, The location of magma chambers at Mt. Etna, Italy, mapped by b-values. *Geophysical Research Letters*, **26**, pp. 2553–2556.

NOIR, J., JACQUES, E., BEKRI, S., ALDER, P.M., TAPPONIER, P. and KING, G.C.P., 1997, Fluid flow triggered migration of events in the 1989 Dobi earthquake sequence of Central Afar. *Geophysical Research Letters*, **24**, pp. 2335–2338.

NUR, A., 1972, Dilatancy, pore fluids, and premonitory variations of ts/tp travel times. *Bulletin of the Seismological Society of America*, **62**, pp. 1217–1222.

NYBLADE, A., PARK, Y., RODGERS, A. and AL-AMRI, A., 2006, Seismic structure of the Arabian Shield Lithosphere and Red Sea Margin. *Margins Newsletter*, **17**, pp. 13–15.

PALLISTER, J.S., MCCAUSLAND, W.A., JÓNSSON, S., LU, Z., ZAHRAN, H.M., HADIDY, S.E., ABURUKBAH, A., STEWART, I.C.F., LUNDGREN, P.R., WHITE, R.A. and MOUFTI, M.R.H., 2010, Broad accommodation of rift-related extension recorded by dyke intrusion in Saudi Arabia. *Nature Geoscience*, **3**, pp. 705–712.

PAROTIDIS, M., ROTHERT, E. and SHAPIRO, S.A., 2003, Pore-pressure diffusion: a possible triggering mechanism for the earthquake swarm 2000 in Vogtland/NW-Bohemia, Central Europe. *Geophysical Research Letter*, **30**, pp. 2075.

PLENEFISCH, T. and KLINGE, K., 2003, Temporal variations of focal mechanisms in the Novy Kostel focal zone (Vogtland/NW-Bohemia)-comparison of the swarms of 1994, 1997 and 2000. *Journal of Geodynamics*, **35**, pp. 145–156.

POWER, J.A., WYSS, M. and LATCHMAN, J.L., 1998, Spatial variations in frequency-magnitude distribution of earthquakes at Soufriere Hills volcano, Montserrat, West Indies. *Geophysical Research Letters*, **25**, pp. 3653–3656.

ROTHERT, E. and SHAPIRO, S.A., 2003, Microseismic monitoring of borehole fluid injections: data modeling and inversion for hydraulic properties of rocks. *Geophysics*, **68**, pp. 685–689.

SCHOLZ, C.H., 2002, *The Mechanics of Earthquakes and Faulting*, 2nd edition (Cambridge, UK: Cambridge University Press).

SCHORLEMMER, D., WIEMER, S. and WYSS, M., 2005, Variations in earthquake-size distribution across different stress regimes. *Nature*, **437**, pp. 539–542.

SHAPIRO, S.A., AUDIGANE, P. and ROYER, J.J., 1999, Large scale in situ permeability tensor of rocks from induced microseismicity. *Geophysical Journal of International*, **137**, pp. 207–213.

SHAPIRO, S.A., HUENGES, E. and BORM, G., 1997, Estimating the crust permeability from fluid-injection-induced seismic emission at the KTB site. *Geophysical Journal of International*, **131**, pp. F15–F18.

SHAPIRO, S.A., ROTHERT, E., RATH, V. and RINDSCHWENTNER, J., 2002, Characterization of fluid transport properties of reservoirs using induced microseismicity. *Geophysics*, **67**, pp. 212–220.

SHAPIRO, S.A., PATZIG, R., ROTHERT, E. and RINDSCHWENTNER, J., 2003, Triggering of seismicity by pore pressure perturbations: permeability related signatures of the phenomenon. *PAGEOPH*, **160**, pp. 1051–1066.

SIGMUNDSSON, F., 2006, Magma does the splits. *Nature*, **442**, pp. 251–252.

STOESER, D.B. and CAMP, V.E., 1985, Pan-African microplate accretion of the Arabian Shield. *Bulletin of the Geological Society of America*, **6**, pp. 817–826.

TSAPANOS, T., 1990, b-value of two tectonic parts in the circum-Pacific belt. *PAGEOPH*, **143**, pp. 229–242.

TZSCHICHHOLZ, F. and WANGEN, M., 1999, *Modellization of Hydraulic Fracturing of Porous Materials*, pp. 227–261 (Southampton, UK: WIT Press).

WANG, H., 2000, *Theory of Linear Poroelasticity* (Princeton, NJ: Princeton University Press).

WIEMER, S., MCNUTT, S.R. and WYSS, M., 1998, Temporal and three-dimensional spatial analysis of the frequency-magnitude distribution near Long Valley caldera, California. *Geophysical Journal of International*, **134**, pp. 409–421.

WIEMER, S., and WYSS, M., 2002, Mapping spatial variability of the frequency-magnitude distribution of earthquakes. *Advances in Geophysics*, **45**, pp. 259–302.

WYSS, M., HASEGAWA, A. and NAKAJIMA, J., 2001, Source and path of magma for volcanoes in the subduction zone of northeastern Japan. *Geophysical Research Letters*, **28**, pp. 1819–1822.

WYSS, M., SHIMAZAKI, K. and WIEMER, S., 1997, Mapping active magma chambers by b-value beneath the off- Ito volcano, Japan. *Journal of Geophysical Research*, **102**, pp. 20413–20422.

YAMASHITA, T., 1999, Pore creation due to fault slip in a fluid permeated fault zone and its effect on seismicity: generation mechanism of earthquake swarm. *Geophysical Journal of International*, **132**, pp. 674–686.

ZAHRAN, H.M., MCCAUSLAND, W.A., PALLISTER, J.S., LU, Z., EL-HADIDY, S., ABURUKBA, A., SCHAWALI, J., KADI, K., YOUSSEF, A., EWERT, J.W., WHITE, R.A., LUNDGREN, P., MUFTI, M. and STEWART, I.C., 2009, Stalled eruption or dike intrusion at Harrat Lunayyir, *Saudi Arabia*? American Geophys. Union, Fall Meeting 2009, abstract #V13E-2072.